J. Chem. Sci. Vol. 124, No. 6, November 2012, pp. 1275–1286. © Indian Academy of Sciences.

Crystallization of organically templated phosphomolybdate cluster-based solids from aqueous solution

MINAKSHI ASNANI, DINESH KUMAR, T DURAISAMY and ARUNACHALAM RAMANAN*

Department of Chemistry, Indian Institute of Technology Delhi, New Delhi 110016, India
e-mail: aramanan@chemistry.iitd.ac.in

Abstract. The paper reports the synthesis and structural characterization of several organic–inorganic solids involving phosphomolybdate clusters. The Strandberg-type $\{P_2Mo_5^{VI}O_{23}\}$ and the lower-valent $\{P_4Mo_6^{V}O_{31}\}$ cluster based solids were isolated in the presence of *en* (ethylenediamine) by controlling pH of the reaction medium. The lower-valent cluster invariably requires the presence of a suitable metal cation for further stabilization. A detailed investigation of the system was carried out where three different weak acids viz. oxalic acid, succinic acid and glycine were used in the entire pH range (1–12). Our results establish that the organic amine (*en*) is alone capable of reducing the molybdenum core in the absence of an organic acid at a suitable pH. Hence, pH of the reaction medium combined with suitable temperature favours the formation of lower-valent phosphomolybdate cluster. Higher pH favours the precipitation of a new sodium hydrogen phosphate.

Keywords. Phosphomolybdate cluster; supramolecular interaction; hydrothermal synthesis.

1. Introduction

Polyoxomolybdate (POM) clusters are attractive nano-sized molecular building blocks for the formation of multi-dimensional organic–inorganic hybrid networks.[1–4] It is always intriguing why multi-component crystals based on phosphomolybdate clusters such as Strandberg-type anion,[5] ($P_2Mo_5O_{23}$), Wells–Dawson anion,[6,7] ($P_2Mo_{18}O_{62}$) and Keggin,[8–10] ($PMo_{12}O_{40}$) precipitate with selected counter cations. The counter cations may vary from simple metal ions (Na, K, Cu) and metal complexes to varying shapes and sizes of organic cations. Like any other solids, these crystals can also show variable stoichiometry (A_mX_n where, m and n are integers) and occur frequently as hydrates of which a few show interesting water oligomers. A common question often raised is whether these are stable crystals that represent free energy minima in the structural landscape of a particular system or non-equilibrium phases. The energy of A_mX_n can be minimized due to either enthalpic or entropic reasons. Enthalpic driven multi-component crystals are generally characterized by distinctive intermolecular interactions like hydrogen bonding. While hydrogen bonds are dominant directive forces in assembling organic cations and POM anions, metal–oxygen coordination is another distinct force in crystallizing metal or metal complex derived polyoxomolybdates. In recent years, weak organic bases and acids are commonly employed as structure directors or templates to control the multi-dimensional frameworks of POM-based solids. The interest mainly stems from the fact that a few of these structurally diverse solids are potential catalysts and proton conductors.[11] Apart from the apparent electrostatic factors, non-covalent interactions operating between the organic cations and inorganic anions contribute significantly to the structural diversity of these solids.[5] In the context of crystal engineering, lately there is considerable interest to rationalize the occurrence of multiple forms (polymorphs, pseudopolymorphs, hydrates/solvates, salts, coordination polymers, etc.) for a crystal obtained from a set of reacting molecules.[12] Formation of a crystalline substance should not be represented by a simple equation as crystallization is a supramolecular reaction.[13] We could employ retrosynthesis,[14] the crystal engineering tool to postulate the possible ways in which tectons or chemically reasonable molecules[15] supramolecularly aggregate before the onset of nucleation by analysing several related crystal structures. Such a hypothesis can provide chemical insights into the occurrence of a particular form. The composition or stoichiometry of the resulting solid, the occurrence of hydration, structural features like water clustering, helicity, etc. may thus become obvious as the mechanistic pathway suggest a link between molecules interacting in the reactant phase and the intermolecular interactions observable in the solid state. In other words, we can make a reasonable assessment of structure–synthesis correlation.

*For correspondence

Our group has successfully employed this approach in several studies.[16]

We have been systematically analysing the crystallization of organic–inorganic salts obtained in the multinary system organic amine - $\{P_2Mo_5O_{23}\}$ - H_2O and perform structure–synthesis correlation using retrosynthesis. The Strandebrg's cluster $\{P_2Mo_5O_{23}\}$ (henceforth referred to as P_2Mo_5) is reasonably a stable cluster anion occurring *in situ* in aqueous solution when a soluble molybdate source is acidified with phosphoric acid over a wide range of pH. Our experience suggests that phosphate to molybdenum molar ratio is hardly a factor to stabilize a particular cluster. A number of salts based on P_2Mo_5 as building blocks is reported in the literature,[17] however, we were the first one to investigate the influence of non-bonding interactions between the organic cations and the Strandberg anion and its influence in the occurrence of water oligomers.[5] In selected cases, we also observed the formation of a reduced phosphomolybdate cluster of the composition ($P_4Mo_6^{V}O_{31}$) forming as a competitive phase at higher temperatures under hydrothermal condition. A combination of organic base that can undergo oxidation and temperature favours the reduction of molybdenum (VI) to lower valent molybdenum (V) species which in turn led to the formation of the reduced phosphomolybdates. Unlike the Strandberg's cluster, this cluster requires further stabilization by a suitable metal ion like Na, Cu, etc. We report here the formation and crystal structures of five Strandberg cluster based salts and four molybdenum (V) based phosphomolybdate solid isolated from the system phosphomolybdate – organic amine – water. A structure–synthesis correlation is attempted based on a tectonic approach.

2. Experimental

2.1 *Synthesis under ambient condition*

Crystallization of multi-component crystals based on POM was attempted from aqueous solution containing a soluble molybdenum source (sodium or ammonium molybdate) and acidified with a weak acid.

2.1a *Synthesis of **1***: In a typical synthesis MoO_3 (0.5 g, 3.5 mmol) was dissolved in morpholine (2.3 mL, 3.5 mmol) in 60 mL of distilled water. H_3PO_4 (0.8 mL, 4.0 mmol) was then added to the resulting grey colour solution to adjust the pH to ~4.0 and was kept at room temperature (25°C) for three months for crystallization. Colourless needle-like crystals were filtered off from the solution and washed with water followed by acetone and dried in air. Yield: 1.2 g, 70% based on molybdenum. Elemental analysis for **1**: C, 3.0;H,1.0; N, 2.0% (Found) and C, 3.2; H,1.0; N,1.8% (Calcd.).

2.1b *Synthesis of **2***: A mixture of $Na_2MoO_4.2H_2O$ (0.5 g, 2.1 mmol) and hexamethylenetetramine (HMTA) (0.453 g, 3.1 mmol) and 60 mL of water were taken in a 150 mL beaker. The pH of the colourless clear solution was adjusted to 4.2 by the addition of H_3PO_4 (0.4 mL, 2.0 mmol). The resulting light brown solution was kept at room temperature (25°C) for two months; colourless crystals were filtered off and washed with water and acetone. Yield: 2.2 g, 65% based on molybdenum. Elemental analysis for **2**: C, 5.6; H, 1.0; N, 3.9% (Found) and C, 6.0; H,1.0; N, 4.0% (Calcd).

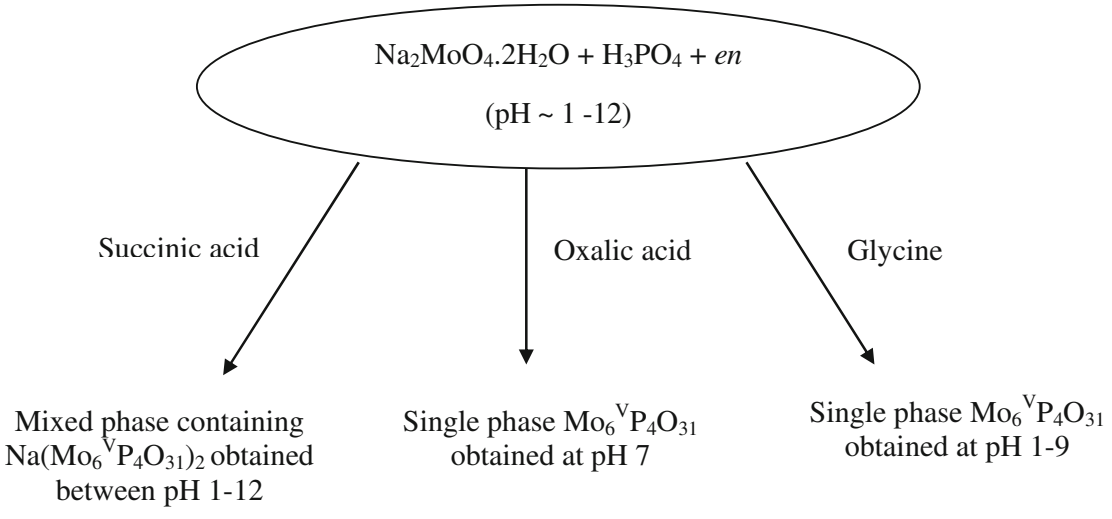

Scheme 1. Schematic representation of synthetic strategy employed.

2.1c *Synthesis of* **3–10**: We later employed ethylenediamine as a template. Oxalic or succinic acids were preferred over acetic acid. Also, at higher pH, glycine was preferred. In a typical synthesis, $Na_2MoO_4.2H_2O$ (0.6217 g, 2.57 mmol), *en* (0.2 mL, 3.22 mmol) and organic template {oxalic acid, succinic acid and an amino acid, glycine (0.6215 g, 4.93 mmol)} were taken in a molar ratio 1:1.25:2 in 15 mL of H_2O in a teflon lined stainless steel container. Adequate amount of H_3PO_4 (1M) was added to this reaction to provide phosphate source and to adjust pH. The reactants were heated at 150°C for two days and then cooled to room temperature. The product obtained was filtered, washed with distilled water followed by acetone and dried in air. Effect of pH and organic acid on the formation of various structures was also investigated extensively.

We varied the stoichiometries of molybdenum source and the counter organic (organic base) with an objective to obtain crystalline products. At times, good crystals were obtained only after several days or weeks. Instantaneous precipitation by rapid evaporation invariably led to X-ray amorphous products or multiphasic mixtures.

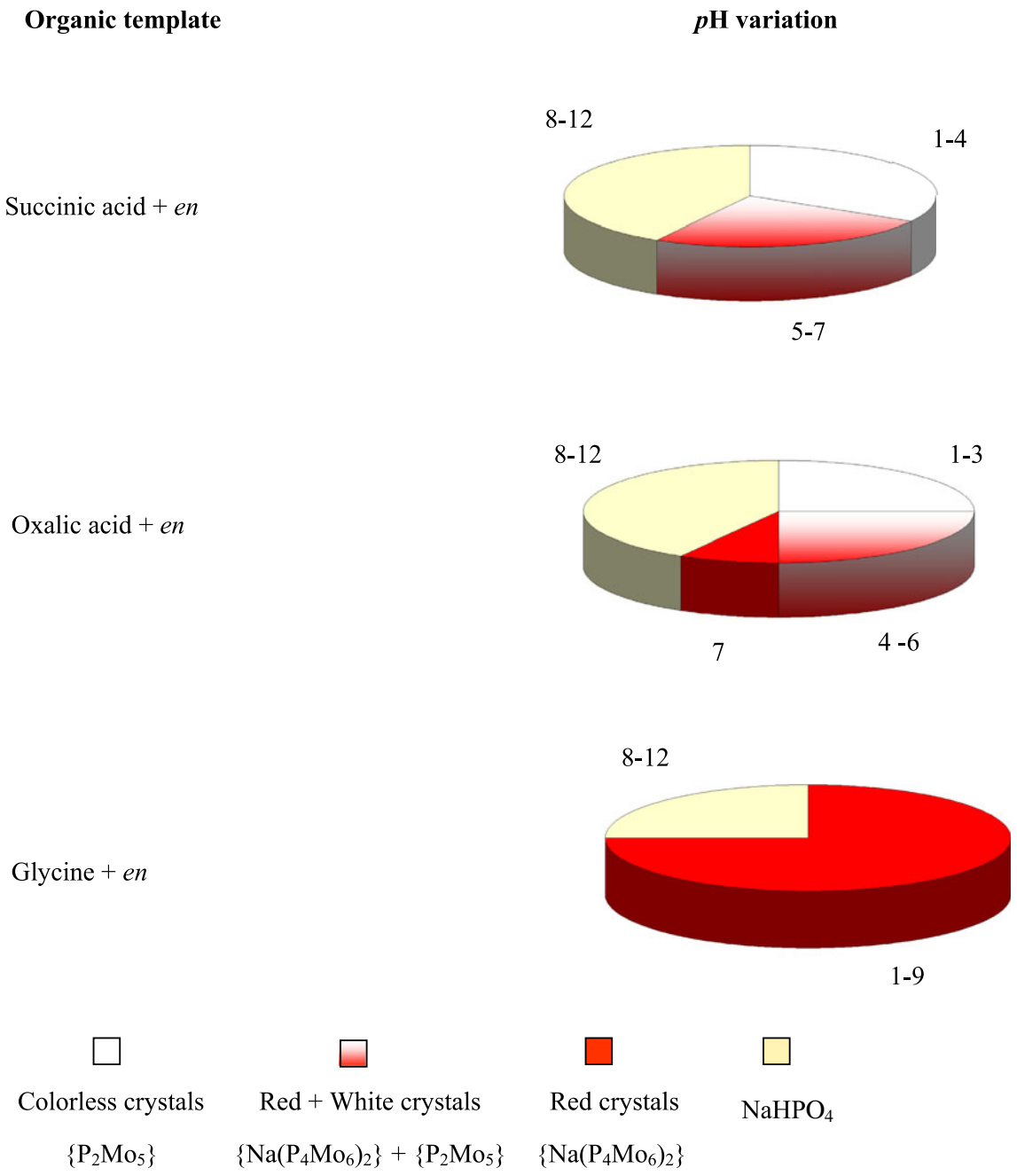

Scheme 2. Influence of different organic templates at varying pH.

Table 1. Crystallographic data for solids **1**–**5**.

	1	**2**	**3**	**4**	**5**
Empirical formula	$C_{20}H_{60}Mo_5N_5O_{33}P_2$	$C_{14}H_{44}Mo_5N_8O_{29}P_2$	$Mo_5P_2O_{23}C_4N_4H_{22}$	$Mo_5P_2O_{32}C_5N_5H_{59}$	$Mo_5P_2O_{26}C_{12}N_{12}H_{64}$
Formula weight	1430.29	1328.20	1035.90	2271.86	1119.81
Temperature (K)	298(2)	298(2)	298(2)	298(2)	298(2)
Space group	$P2_1$	$P\bar{1}$	$C2/c$	$P2_1/c$	$P\bar{1}$
a (Å)	14.1882(2)	12.1142(2)	17.609(3)	13.8369(9)	8.9537(7)
b (Å)	8.4175(1)	13.2522(2)	9.9742(13)	34.482(2)	10.6146(8)
c (Å)	18.7080(1)	14.9194(2)	13.7422(17)	12.8923(8)	17.4236(14)
α (°)	90.00	89.761(1)	90.00	90.00	78.77(0)
β (°)	90.285(1)	77.245(1)	96.826(3)	101.803(1)	92.713(2)
γ (°)	90.00	64.291(1)	90.00	90.00	67.32(0)
V (Å^3)	2234.25(4)	2093.34(3)	2396.6(6)	6021.1(7)	1490.31(20)
Z	2	2	4	4	1
D_{calc}, (g cm^{-3})	2.126	2.107	2.871	2.506	2.651
Goodness-of-fit (GOF) on F^2	1.023	1.085	1.105	1.010	1.169
λ (Å)	0.71073	0.71073	0.71073	0.71073	0.71073
R_1, wR_2 [$I > 2\sigma(I)$][a]	0.0259, 0.0685	0.0308,0.0924	0.0294, 0.0771	0.0441, 0.0965	0.0397, 0.1067
$\Delta\rho_{max}$ and $\Delta\rho_{min}$ (e Å^{-3})	0.631 and −0.674	-	0.772 and −1.573	1.065 and −0.935	0.923 and −0.909
CCDC	229195	-	863392	863393	863391

Yields vary between 30 and 60% in most of the studies based on molybdenum. Schemes 1 and 2 briefly describe the synthetic protocol employed and influence of different organic templates at varying pH in this study.

2.2 *X-ray crystallographic studies*

X-ray diffraction study of a crystal mounted on a capillary was carried out on a BRUKER AXS SMART-APEX diffractometer with a CCD area detector (Kα:

Table 2. Crystallographic data for solids **6**–**10**.

	6	**7**	**8**	**9**	**10**
Empirical formula	$Mo_6P_4O_{43}Na_1C_{14}N_{14}H_{93}$	$Mo_{12}P_8O_{67}Na_2C_{12}N_{12}H_{80}$	$Mo_6P_4O_{39}Na_1C_{14}N_{14}H_{87}$	$Mo_6P_4O_{49}Na_1C_4N_4H_{116}$	$Na_2P_2O_{14}C_2N_2H_{17}$
Formula weight	2606.03	2829.26	1483.02	3232.28	415.08
Temperature(K)	298(2)	298(2)	298(2)	298(2)	298(2)
Space group	$P2_1$	$P\bar{1}$	$P\bar{1}$	$P4/ncc$	$P2_1/c$
a (Å)	13.223(3)	12.0528(7)	11.7833(11)	27.1919(7)	11.739(3)
b (Å)	16.612(4)	14.6366(9)	13.3689(12)	27.1919(7)	10.193(2)
c (Å)	18.867(5)	21.3482(13)	14.5752(13)	28.2835(10)	6.8574(15)
α (°)	90.00	80.6570(10)	68.548(2)	90.00	90.00
β (°)	96.574(5)	82.6650(10)	74.5030(10)	90.00	105.071(3)
γ (°)	90.00	76.3050(10)	65.772(2)	90.00	90.00
V (Å^3)	4117.2(18)	3594.8(4)	1930.1(3)	20912.8(11)	792.3(3)
Z	2	2	2	8	4
D_{calc}, (g cm^{-3})	2.102	2.614	2.552	2.053	1.719
Goodness-of-fit (GOF) on F^2	1.025	1.039	0.978	1.038	1.096
λ (Å)	0.71073	0.71073	0.71073	0.71073	0.71073
R_1, wR_2 [$I > 2\sigma(I)$][a]	0.1009, 0.2623	0.0391, 0.1134	0.0439, 0.1081	0.0606 - 0.1891	0.0412, 0.1081
$\Delta\rho_{max}$ and $\Delta\rho_{min}$ (e Å^{-3})	0.923 and −0.909	2.134 and −2.024	1.307 and −1.373	2.513 and −1.571	0.538 and −0.276
CCDC	863395	863394	863396	863397	864249

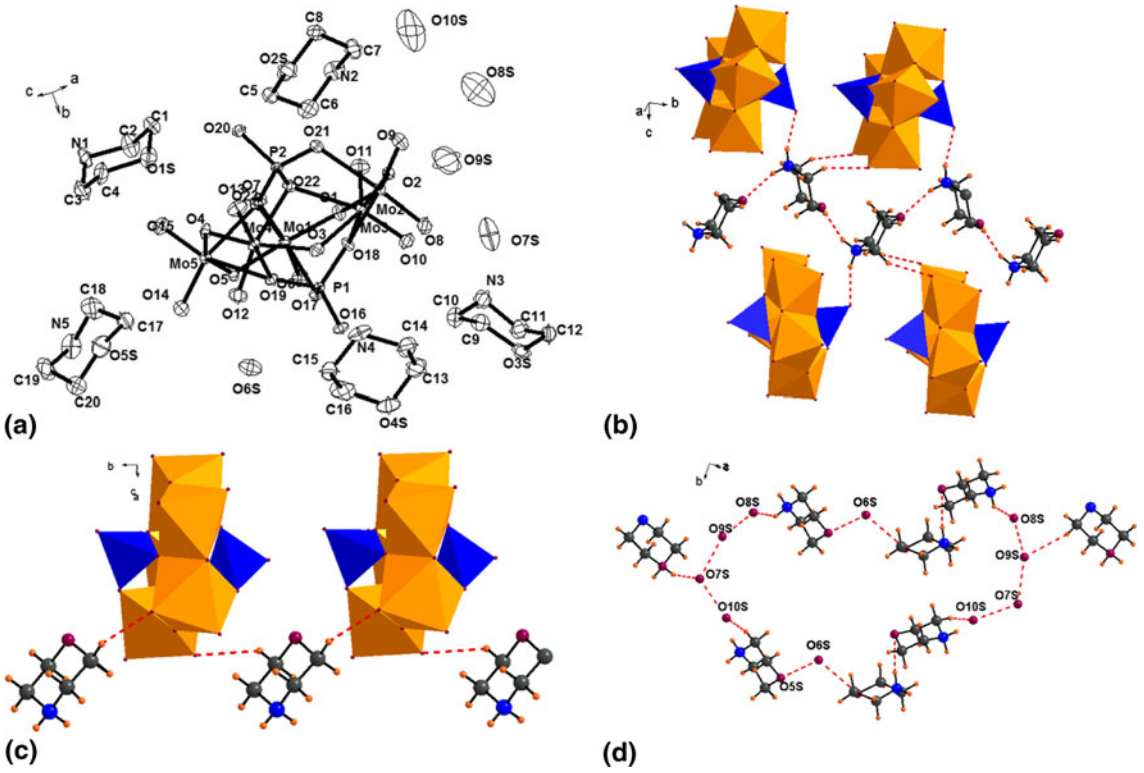

Figure 1. (**a**) ORTEP view of asymmetric unit of solid **1**. Thermal ellipsoids are drawn at 50% probability level. (**b**) Zig-zag arrangement of morpholinium cations with cluster. (**c**) 1–D chain of cluster with counter cation as morpholinium ions. (**d**) There is appreciable hydrogen bonding only between the morpholinium ions and the space filling water molecules.

0.71073 Å, monochromator: graphite).[18] Frames were collected at T = 298 K by ω, ϕ and 2θ –rotation at 10 s per frame with SAINT.[19] The measured intensities were reduced to F^2 and corrected for absorption with SADABS.[19] Structure solution, refinement, and data output were carried out with the SHELXTL program.[20] Non-hydrogen atoms were refined anisotropically. C–H hydrogen atoms were placed in geometrically calculated positions by using a riding model. O–H hydrogen atoms were localized by difference Fourier maps and refined in subsequent refinement cycles. Images were created with the DIAMOND program.[21] Hydrogen bonding interactions in the crystal lattice were calculated with SHELXTL and DIAMOND.[20,21] The crystal data and structure refinement of solids **1–5** and **6–10** are summarized in tables 1 and 2, respectively.

3. Results and discussion

3.1 *Crystal structures of monoamine derived HP_2Mo_5 solids (**1** and **2**)*

The crystal structure of **1**, $[(C_4H_{10}NO)_5][HP_2Mo_5O_{23}].5H_2O$, is made of monoprotonated cluster HP_2Mo_5 and morpholinium cations. N–H· · ·O and C–H· · ·O interactions (supplementary table S1) aggregate the cations and anions on a sheet (figure 1). The structure also shows strong interactions between the organic cations and mediating water molecules as observed in our earlier study.[5]

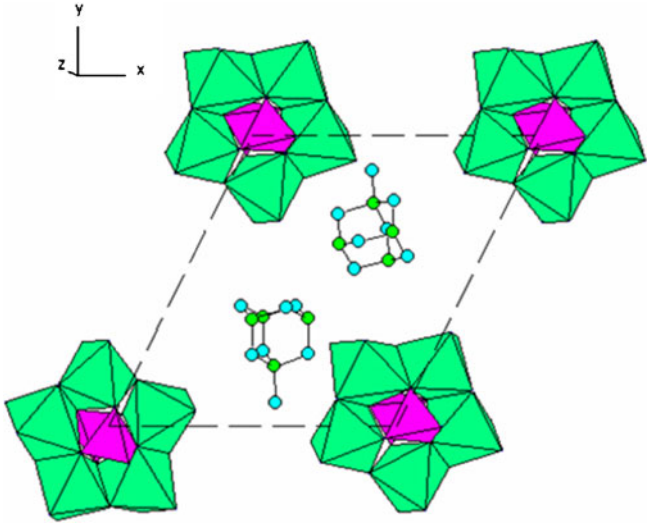

Figure 2. Me–HMTA forming packing with cluster through H-bonding in solid **2**.

The crystal structure of **2**, [(HMTA-Me)$_2$][$H_4P_2Mo_5O_{23}$].6H_2O, is made of tetraprotonated cluster $H_4P_2Mo_5$ and HMTA-Me (HMTA = Hexamethylenetetramine) cations with space-filling water molecules. In **2**, C–H· · ·O (figure 2) interactions are responsible for seggregation of the cluster and organic cations.

3.2 *Crystal structures of diamine derived $H_2P_2Mo_5$ solids (**3**, **4** and **5**)*

3.2a *Phase diagram of en– phosphomolybdate – H_2O system*: Crystallization was performed over the entire pH range (1–12) in the presence of *en* but different weak

Table 3. Experimental condition and type of tectons of solids **1**–**5**.

Sample code	Composition	Temperature/pH	Tectons
1	[($C_4H_{10}NO)_5$][$HP_2Mo_5O_{23}$].5H_2O	RT, pH = 4	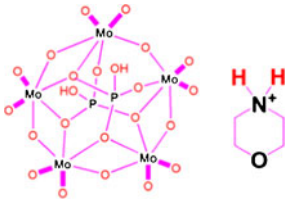
2	[(HMTA-Me)$_2$] [$H_4P_2Mo_5O_{23}$].6H_2O	RT, pH = 4.2	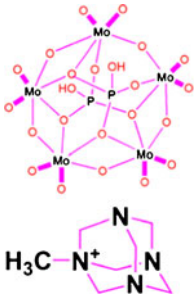
3	(*en*$H_2)_2$[$H_2P_2Mo_5O_{23}$]	150°C, pH = 1	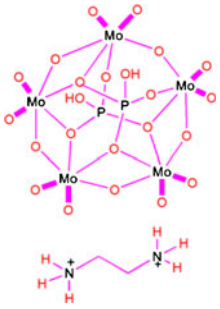
4	(*en*$H_2)_2$(*en*)$_{0.5}$[$H_2P_2Mo_5O_{23}$].9H_2O	150°C,pH = 3	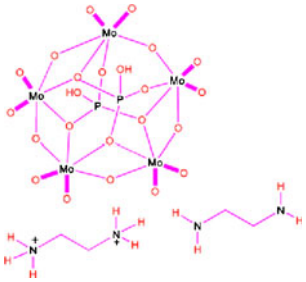
5	(*en*H_2)(*en*H)$_2$[$H_2P_2Mo_5O_{23}$].3H_2O	150°C, pH = 5–7	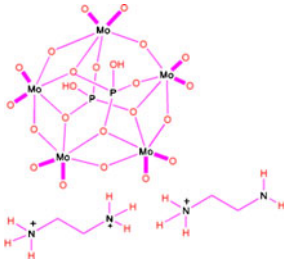

organic acids. Scheme 2 shows the formation of three types of products based on colour depending on the pH range. In the pH range 5–7, the products were biphasic mixture containing white **5** and red **7** crystals.

At very low pH (pH = 1), an anhydrous solid **3**, $(enH_2)_2[H_2P_2Mo_5O_{23}]$ was obtained. The crystal packing of **3** is made of two tectons, enH_2 and $H_2P_2Mo_5$ cluster (table 3). Adjacent clusters are bridged by a pair of enH_2 cations through strong N–H· · ·O interactions (figure 3) (supplementary table S1). The solid **4**, $(enH_2)_2(en)_{0.5}[H_2P_2Mo_5O_{23}].9H_2O$ is another multicomponent crystal derived from enH_2 and $H_2P_2Mo_5$ tectons. Also, water molecules mediate the building of this complex solid (figure 4). Analysis of colourless crystals isolated at pH = 5–7 indicated the presence of **5**. The crystal structure of **5**, $(enH_2)(enH)_2[H_2P_2Mo_5O_{23}].3H_2O$, consists of the diprotonated Strandberg cluster and two types of protonated ethylenediammonium cations. A significant structural feature is that of P_2Mo_5 cluster being linked into chains through mediating water molecules. The chains are further linked through diprotonated enH_2 forming 2–D sheets (figure 5b).

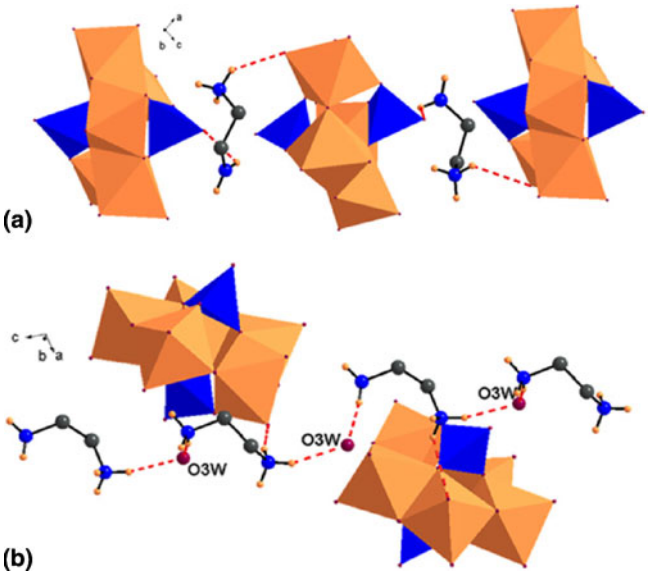

Figure 4. (**a**) 1–D chain among enH_2 and $P_2Mo_5O_{23}$ cluster through the H-bonding. (**b**) 1–D chain of **4** through the H-bonding of (enH_2) N–H· · ·Ow· · ·H–N (enH_2) and (enH_2) N–H· · ·O–Mo.

3.3 *Crystal structures of diamine derived P_4Mo_6 solids (**6**, **7**, **8** and **9**)*

Crystallization under hydrothermal condition at higher temperatures were favourable for the reduction of molybdenum(VI) to molybdenum(V) resulting in another fully reduced phosphomolybdate cluster, $\{P_4Mo_6^VO_{31}\}$.

Structural analysis of all the red crystals **6–8** showed the presence of $\{P_4Mo_6^VO_{31}\}$ clusters as one of the building blocks along with ethylenediammonium and sodium cations. We carried out bond valence sums (BVS) to ascertain the nature of protonation of *en* and the clusters. BVS of **6** revealed six protonated μ_2-O atoms and fourteen protonated terminal P–O atoms. Hence, every cluster has six $Mo_5(OH)_3$, one $PO_3(OH)$ and three $P(OH)_2$ units (table 4). Hence the composition of **6** was assigned to be $(en)_4(enH)_3[Na\{H_{10}P_4Mo_6O_{31}\}_2].12H_2O$. This is in accordance with the cases of **7** and **8**, where the P_4Mo_6 units constituting a dimer have the same sites of protonation. The $Na(P_4Mo_6)_2$ dimers are formed by crystallographically different Mo, P and O atoms. Unlike **7** and **8**, where {A-Na(1)-A} type of dimers formed by crystallographically identical P_4Mo_6 clusters were observed, **6** consists of {A-Na(1)-B} type of dimers (figure 6). Both solids **7**, $(enH_2)(enH)_5Na_2[H_{15}\{P_4Mo_6O_{31}\}_2(H_2O)].4H_2O$ and **5** were found in the same reaction. The structure is a beautiful assembly of sodium bridged lower-valent phosphomolybdate cluster interacting through Na–O–P to form a 3–D structure (figure 7). BVS analysis of **8** suggested that three μ_2-O atoms and five terminal P–O atoms are protonated. The composition of the solid was deduced as $(enH)_7[Na\{H_8P_4Mo_6O_{31}\}_2].8H_2O$. Two P_4Mo_6 clusters are linked through six μ_2-O atoms [O(1), O(2), O(4)] to Na(1) cations to form $[Na(1)(P_4Mo_6)]_2$ dimer (figure 8). The octahedral coordination around Na(2) is completed by two water molecules. Strong H-bonding interactions (supplementary table S1) involving cluster anions, enH_2 and water molecules occur in the structure. Although both **7** and

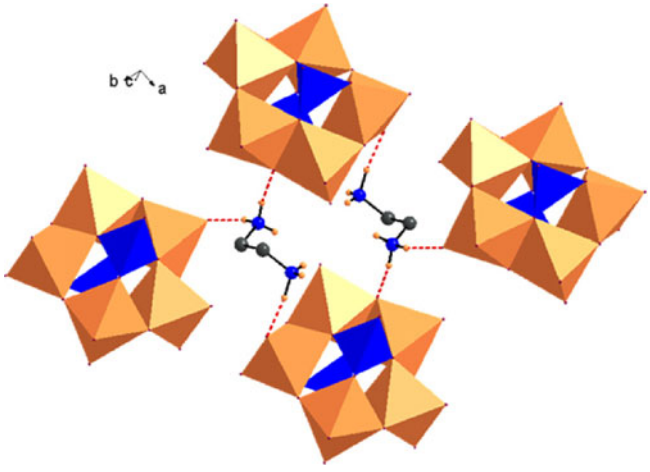

Figure 3. 2–D sheet of $(enH_2)_2[H_2P_2Mo_5O_{23}]$, **3** through the H-bonding of N–H· · ·O–Mo.

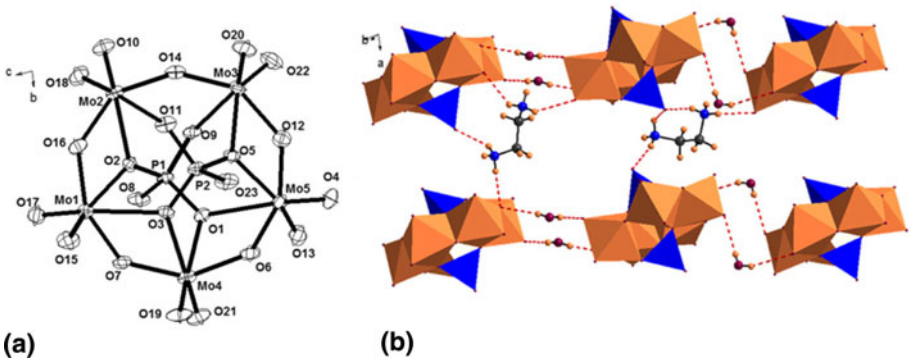

Figure 5. (**a**) ORTEP view of cluster P_2Mo_5 in **5**. Thermal ellipsoids are drawn at 50% probability level. (**b**) 2–D sheet of $(enH_2)(enH)_2[H_2P_2Mo_5O_{23}].3H_2O$, **5** through the hydrogen bonding of Ow–H· · ·O–Mo, N–H· · ·O–Mo and N–H· · ·O–P.

Table 4. Experimental condition and type of tectons of solids **6**–**10**.

Sample code	Composition	Temperature/pH	Tectons
6	$(en)_4(enH_2)_3[Na\{H_{10}P_4Mo_6O_{31}\}_2].12H_2O$	150°C, pH = 5	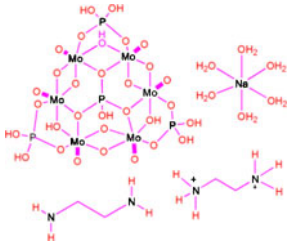
7	$(enH_2)(enH)_5Na_2[H_{15}(P_4Mo_6O_{31})_2(H_2O)].4H_2O$	150°C, pH = 5–7	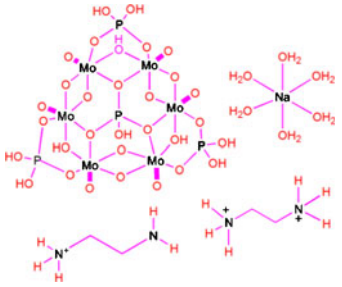
8	$(enH)_7[NaH_8P_4Mo_6O_{31}].8H_2O$	150°C, pH = 7	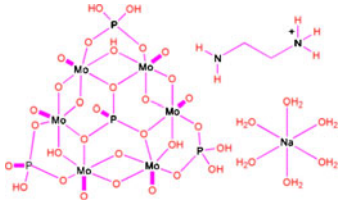
9	$(enH)(enH_2)[Na\{H_{10}P_4Mo_6O_{31}\}_2].18H_2O$	150°C, pH = 8	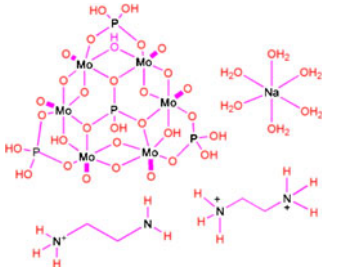
10	$(enH_2)_{0.5}[NaHPO_4].3H_2O$	150°C, pH = 8–12	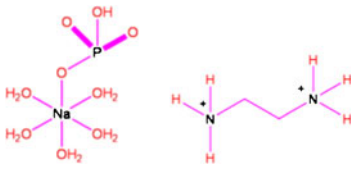

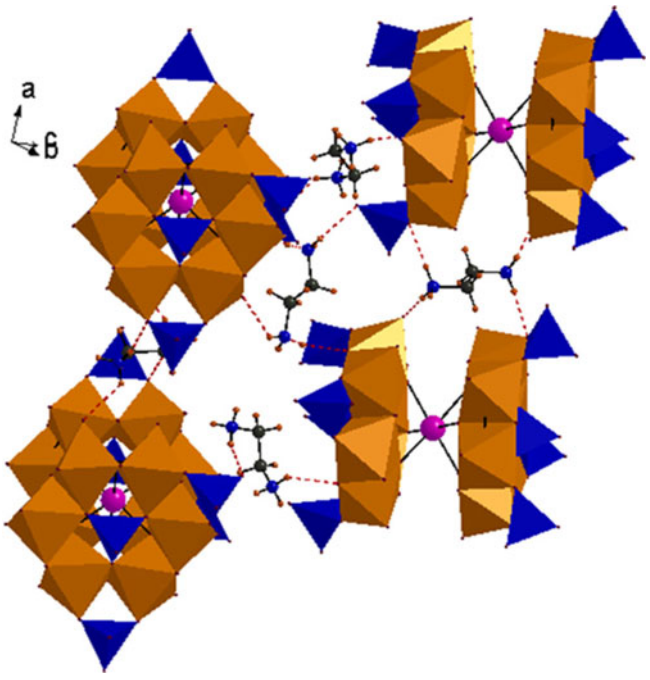

Figure 6. H-bonding occurring between the dimeric anions and organic cations in **6**. Water molecules are omitted for clarity.

8 are based on $Na(P_4Mo_6)_2$ dimeric unit, the two structures differ considerably. While in **7**, two kinds of dimers, $[Na(1)(P_4Mo_6)]_2$ and $[Na(2)(P_4Mo_6)]_2$, differing in protonation were observed while in **8** only one type occurred. In this context, $[Na(1)(P_4Mo_6)]_2$ dimer occurring in **8** was similar to $[Na(2)(P_4Mo_6)]_2$ observed in **7** containing the same number of protonated atoms. In addition, **7** possesses a layered structure, **8** consists of 1–D chains of $Na(P_4Mo_6)_2$ dimers. In contrast to almost orthogonal disposition of dimeric units in **7**, a unidirectional alignment of such units was encountered in **8**.

At pH 8, another solid containing P_4Mo_6 cluster, $(enH)(enH_2)[Na\{H_{10}P_4Mo_6O_{31}\}_2].18H_2O$ (**9**) was isolated. This structure showed the largest unit cell obtained in our system. The compound **9** consists of P_4Mo_6 cluster with three $P(OH)_2$ and one $PO_3(OH)$ group along with three μ_2-OH units. Such protonation has been encountered in **7** but here the clusters have been linked through Na^+ to form {A-Na-A} dimer

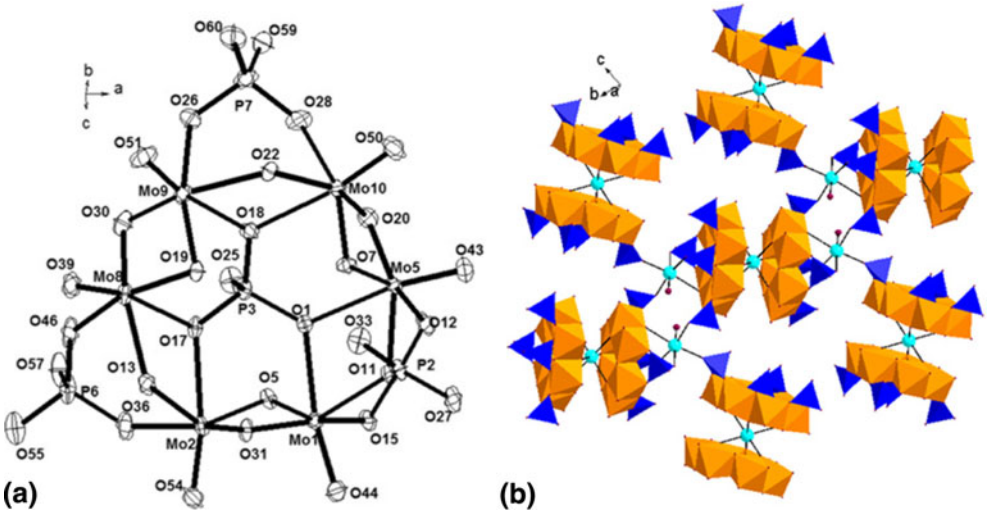

Figure 7. (**a**) ORTEP view of cluster P_4Mo_6 in **7**. Thermal ellipsoids are drawn at 50% probability level. (**b**) View of channels along [001]. The organic cations and water molecules have been omitted for clarity.

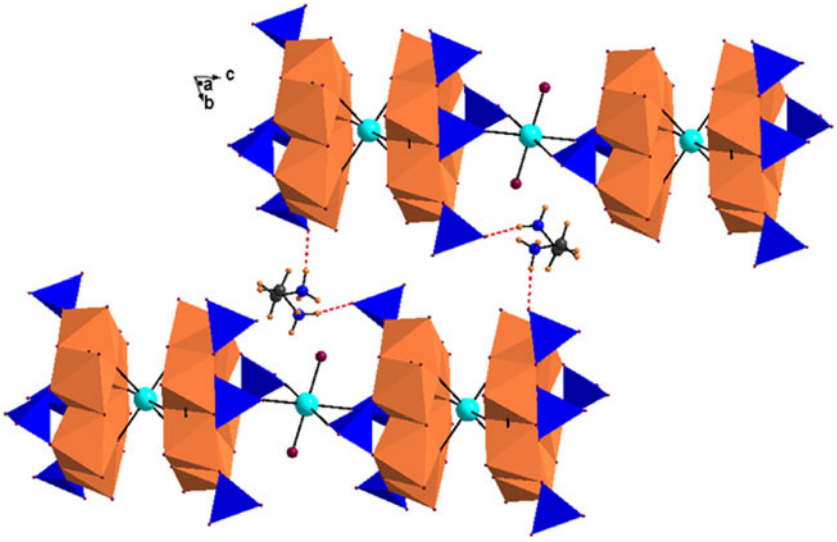

Figure 8. $Na[P_4Mo_6]_2$ dimer linking two P_4Mo_6 units connected through NaO_6 octahedra and P–O· · ·H–N(*en*H) forming 2–D chains in **8**.

rather than {A-Na-B} type. The dimers are arranged in an orthogonal mode with respect to the nearest neighbour. In addition to the organic cations and water molecules, a tetrahedral phosphate group also exists in the structure. The structure exhibits complex H-bonding interactions (supplementary table S1) involving

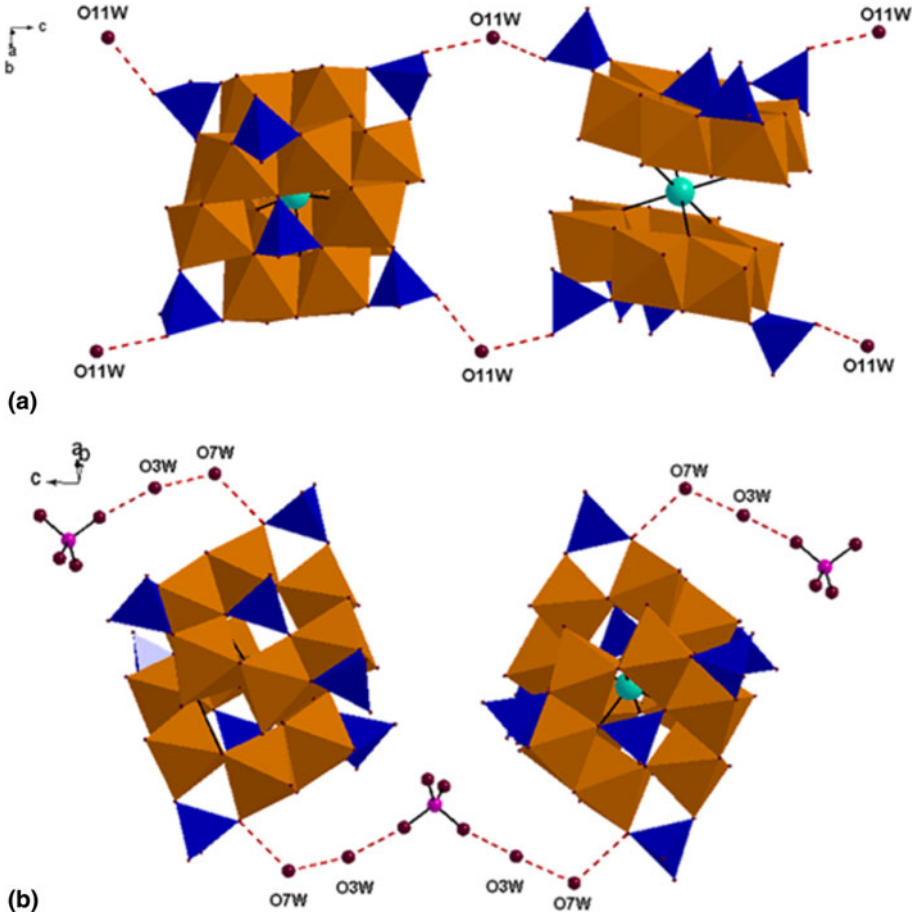

Figure 9. (**a**) 1–D chain form through the P–O· · ·Ow· · ·O–P interactions in solid **9**. (**b**) Zig-zag chain is form through PO_4 and water interactions with cluster.

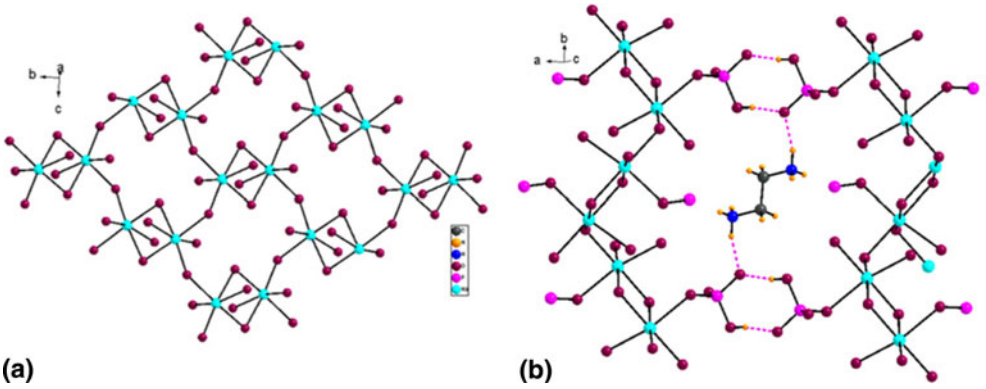

Figure 10. (**a**) 2–D sheets of hydrated Na water bridge dimer in **10**. (**b**) 2–D sheet through the N–H· · ·O–P and P–H· · ·O–P interaction in **10**.

the anionic dimers, organic cations, water molecules and phosphate group (figure 9).

Under strong alkaline conditions (pH > 8) long, white needle-shaped crystals of $(enH_2)_{0.5}[NaHPO_4].3H_2O$, **10** were isolated. The solid is an unusual salt of ethylenediammonium incorporated sodium hydrogen phosphate. Retrosynthesis of **10** suggested that the beautiful assembly is built from the condensation of the tectons, a water-bridged dimer $\{Na_2(H_2O)_{10}\}$ and monoprotonated phosphate, $\{HPO_4\}$ (table 4). The condensation on *bc*-plane led to the interaction of sodium hydrate dimers to form a 2–D sheet of the composition $\{Na(H_2O)_3(HPO_4)\}^-$. The dimers are linked to each other through water bridges. The sheets are connected to each other through the complementary interactions (supplementary table S1), P–H· · ·O–P as shown in figure 10. The counter cations enH_2 occurs in the cavities and connect the monophosphates through N–H· · ·O (figure 10b).

4. Analysis of molybdenum phosphate hybrid solids

The FTIR spectra observed for **1** and **2** associated with Mo_5 ring were similar. The strong intensity bands at 950, 900, 875 and 850 cm^{-1} are due to $\nu_{Mo=O}$ for the different molybdenum environments. The features at 750, 700, 600 and 530 cm^{-1} are attributed to the symmetric and asymmetric stretching modes of the molybdate ring, Mo_5O_{15}, while a band ∼1040 cm^{-1} is due to the terminal P–O of the capped phosphate sites. The bands at 3020, 2880, 2500, 1650, 1500, 1340 and 1100 cm^{-1} and 3177, 1634, 1465, 1400, 1260, 1150 and 1100 cm^{-1} are in the characteristic region of the organic groups of the compounds **1** and **2**, respectively. The solids from **3–10** have been characterized by various analytical techniques. FTIR spectra of compounds exhibit a strong band at 952 cm^{-1}, characteristic of ν(M=O) and features at 733 and 1038 cm^{-1} associated with ν(Mo–O–Mo) and ν(P–O), respectively. The features at 3493, 3026 and 1522 cm^{-1} are characteristic of enH_2, while other strong features at 3368 and 1577 cm^{-1} are assigned to water molecules.

5. Chemistry of formation of phosphomolybdate cluster-based solids

In this study, we have isolated several new crystals based on phosphomolybdate clusters. A detailed investigation of the system was carried out where synthesis was carried out in the presence of three different organic acids viz. oxalic acid, succinic acid and glycine (an amino acid) in the entire pH range (1–12). Although organic acids were not incorporated in the structure of solids, they appear to influence the crystallization. A combination of powder and single crystal XRD clearly establishes that only a few solids crystallize under varying pH. The present investigation unambiguously proved that a combination of *en* along with a suitable pH and temperature is essential to obtain the reduced cluster $\{P_4Mo_6^{V}O_{31}\}$. The cluster $\{P_4Mo_6\}$ is a very stable species that is formed under a myriad of synthetic conditions and is the basis of numerous and diverse group of phosphomolybdates.[22] The cluster has not been observed in the absence of metal cations. It is significant that in most of the structures, dimerization occurs through linking with a transition metal ion and solids based on exclusively linkage with sodium ion are rare. In this context, the present work is a significant contribution where $\{P_4Mo_6\}$ dimers linked with sodium cation led to the isolation of structures with varying dimensionality. It is noteworthy that when the reactions were performed in the presence of the three selected organic acids (viz. succinic acid, oxalic acid and glycine) under ambient conditions, reduction of molybdenum core was not effected

at any pH. This observation establishes that temperature (indirectly hydrothermal condition) is critical to form reduced phosphomolybdates.

6. Conclusions

The system of reduced phosphomolybdates was investigated extensively under hydrothermal conditions. Three P_2Mo_5, four $Na(Mo_6P_4)_2$ and $NaHPO_4$ based solids were obtained by varying pH as well as organic template (succinic acid, oxalic acid and glycine). The dimensionality of phosphomolybdates framework was found to be controllable to a considerable extent by reaction parameters such as pH and organic template. This confirms the strong ability of hydrothermal technique for the preparation of new organic–inorganic hybrid materials.

Supplementary material

For supplementary information (table S1), see www.ias.ac.in/chemsci website.

Acknowledgements

DK acknowledges the Department of Science and Technology (DST), New Delhi for Research Fellowship. AR acknowledges the DST for providing continuous funding for the past two decades and infrastructural support.

References

1. Singh M and Ramanan A 2011 *Cryst. Growth Des.* **11** 3381; (b) Singh M, Loftland S E, Ramanujachary K V and Ramanan A 2011 *Cryst. Growth Des.* **10** 5105
2. Dolbecq A, Dumas E, Mayer C R and Mialane P 2010 *Chem. Rev.* **110** 6009
3. Müller A, Peters F, Pope M T and Gatteschi D 1998 *Chem. Rev.* **98** 239
4. (a) Pope M T and Müller A 1994 *Polyoxometalates: From platonic solids to anti-retroviral activity* (Dordrecht: Kluwer Academic Publishers); (b) Cindriæ M, Veksli Z and Kamenar B 2009 *Croat. Chem. Acta* **82** 345; (c) Yamase T 1993 *Mol. Eng.* **3** 241; (d) Kortza U, Müller A, Slageren J V, Schnacke J, Dalal N S and Dressel M 2009 *Coord. Chem. Rev.* **253** 2315
5. (a) Thomas J and Ramanan A 2008 *Cryst. Growth Des.* **8** 3390; (b) Upreti S and Ramanan A 2005 *Acta Cryst.* **E61** m414; (c) Upreti S and Ramanan A 2008 *Synth. React. Inorg., Met.-Org., Nano-Met. Chem.* **38** 69; (d) Upreti S and Ramanan A 2006 *Cryst. Growth Des.* **6** 2066; (e) Thomas J and Ramanan A 2011 *Inorg. Chim. Acta* **372** 243
6. Bareyt S, Piligkos S, Hasenknopf B, Gouzerh P, Lacôte E, Thorimbert S and Malacria M 2005 *J. Am. Chem. Soc.* **127** 6788
7. Niu J Y, Guo D J, Wang J P and Zhao J W 2004 *Cryst. Growth Des.* **4** 24
8. Zheng P Q, Ren Y P, Long L S, Huang R B and Zheng L S 2005 *Inorg. Chem.* **44** 1190
9. Ren Y P, Kong X J, Long L S, Huang R B and Zheng L S 2006 *Cryst. Growth Des.* **6** 572
10. Ren Y P, Kong X J, Hu X Y, Sun M, Long L S, Huang R B and Zheng L S 2006 *Inorg. Chem.* **45** 4016
11. Dey C, Kundu T and Banerjee R 2012 *Chem. Commun.* **48** 266
12. Desiraju G R, Vittal J J and Ramanan A 2011 *Crystal engineering — A textbook* (Singapore: World Scientific Press)
13. Desiraju G R 2007 *Angew. Chem.* **46** 8342
14. (a) Singh M, Thomas J and Ramanan A 2010 *Aust. J. Chem.* **63** 1; (b) Pavani K, Singh M and Ramanan A 2011 *Aust. J. Chem.* **64** 68; (c) Singh M, Kumar D, Thomas J and Ramanan A 2010 *J. Chem. Sci.* **122** 757
15. Tectons (the Greek word $\tau\varepsilon\kappa\tau\omega\nu$ for builder) are chemically reasonable molecules that induce supramolecular aggregation through controlled geometry. These vary from simple molecules such as H_2O to robust units such as metal complexes; (a) Nangia A 2004 *Nomenclature in crystal engineering in encyclopedia of supramolecular chemistry* (United Kingdom: CRC Press); (b) Brunet P, Michel S and Wuest J D 1997 *J. Am. Chem. Soc.* **119** 2737
16. (a) Pavani K, Singh M, Ramanan A, Lofland S E and Ramanujachary K V2009 *J. Mol. Struct.* **933** 156; (b) Pavani K and Ramanan A 2005 *Eur. J. Inorg. Chem.* 3080; (c) Thomas J, Agarwal M, Ramanan A, Chernova N and Whittingham M S 2009 *Cryst. Eng. Commun.* **11** 625; (d) Upreti S, Datta A and Ramanan A 2007 *Cryst. Growth Des.* **7** 966
17. (a) He X, Zhang P, Song T-U, Mu Z-C, Yu J-H, Wang Y and Xu J-N 2004 *Polyhedron* **23** 2153; (b) Burkholder E, Golub V, O'Connor C J, and Zubieta J 2003 *Inorg. Chem.* **42** 6729; (c) Lu J, Xu Y, K N, Goh and Chia L S 1998 *Chem. Commun.* 2733; (d) Meng J X, Lu Y, Li Y G, Fu H and Wang E B, 2011 *Cryst. Eng. Commun.* **13** 2479
18. Bruker Analytical X-ray Systems 2000 *SMART: Bruker molecular analysis research tool, Version 5.618*
19. Bruker Analytical X-ray Systems 2001 *SAINT-NT, Version 6.04*
20. Bruker Analytical X-ray Systems 2000 *SHELXTL-NT, Version 6.10*
21. Klaus B 1999 *DIAMOND, Version 1.2c* (Germany: University of Bonn)
22. Zhang L, Li X, Zhou Y and Wang X 2009 *J. Mol. Struct.* **928** 59; (b) Khan M I, Chen Q and Zubieta J 1995 *Inorg. Chim. Acta* **235** 135; (c) Ma Y, Li Y, Wang E, Lu Y, Wang X and Xu X 2007 *J. Coord. Chem.* **60** 719; (d) Streb C, Long D L and Cronin L 2007 *Chem. Commun.* 471; (e) Streb C, Long D L and Cronin L 2006 *Cryst. Eng. Commun.* **8** 629; (f) Xu L, Sun Y, Wang E, Shen E, Liu Z, Hu C, Xing Y, Lin Y and Jia H 1999 *J. Solid State Chem.* **146** 533